



BELL NONLOCALITY AND COLLIDER STUDIES

Zhijie Zhao

zhao@physik.uni-siegen.de

April 22, 2025

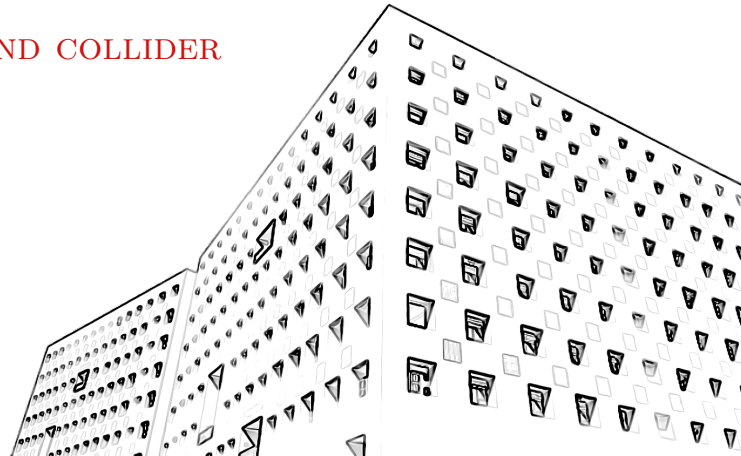




Table of Contents

1 Bell nonlocality

► Bell nonlocality

► Methodology

► Collider studies

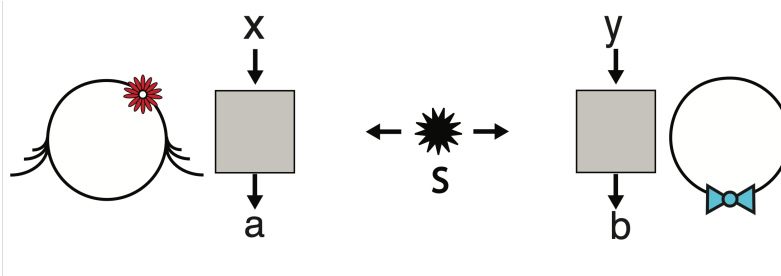
► Summary



Alice and Bob

1 Bell nonlocality

A typical “Bell experiment” can be depicted by this image:



N. Brunner *et al.*, arXiv:1303.2849

- Alice and Bob are two observers of a common source S .
- Alice choose x to measure, and the output is A .
- Bob do the similar measurement by y , where the output is B .
- The outcomes are described by a probability distribution $p(AB|xy)$.



Alice and Bob

1 Bell nonlocality

In this experiment, a particle is decayed to two spin- $\frac{1}{2}$ particles. One of them fly to Alice, and the other fly to Bob. Because of the correlation of these particles, we have

$$p(AB|xy) \neq p(A|x)p(B|y),$$

where $p(A|x)$ and $p(B|y)$ are local probability.

Alice and Bob can be separated by a large distance, so this theory is nonlocal. Locality implies there are a set of hidden variables λ , and we have:

$$p(AB|xy, \lambda) = p(A|x, \lambda)p(B|y, \lambda).$$

The λ is characterized by a probability distribution $q(\lambda)$. Finally, we have:

$$p(AB|xy) = \int_{\Lambda} d\lambda q(\lambda) p(A|x, \lambda) p(B|y, \lambda).$$



CHSH inequality

1 Bell nonlocality

For simplicity, we can choose $x, y \in \{1, 2\}$ and $A, B \in \{-1, +1\}$. The expectation value of the product AB is

$$\begin{aligned}\langle A_x B_y \rangle &= \sum_{A,B} AB p(AB|xy) \\ &= \int_{\Lambda} d\lambda q(\lambda) \langle A_x \rangle_{\lambda} \langle B_y \rangle_{\lambda}\end{aligned}$$

where $\langle A_x \rangle_{\lambda} = \sum_A A p(A|x, \lambda)$ and $\langle B_y \rangle_{\lambda} = \sum_B B p(B|y, \lambda)$.

This gives:

$$\langle A_1 B_1 \rangle - \langle A_1 B_2 \rangle = \int_{\Lambda} d\lambda q(\lambda) (\langle A_1 \rangle_{\lambda} \langle B_1 \rangle_{\lambda} - \langle A_1 \rangle_{\lambda} \langle B_2 \rangle_{\lambda})$$



CHSH inequality

1 Bell nonlocality

In the bracket, we can further expand:

$$\begin{aligned}\langle A_1 \rangle_\lambda \langle B_1 \rangle_\lambda - \langle A_1 \rangle_\lambda \langle B_2 \rangle_\lambda &= \langle A_1 \rangle_\lambda \langle B_1 \rangle_\lambda - \langle A_1 \rangle_\lambda \langle B_2 \rangle_\lambda \pm \langle A_1 \rangle_\lambda \langle B_1 \rangle_\lambda \langle A_2 \rangle_\lambda \langle B_2 \rangle_\lambda \\ &\quad \mp \langle A_1 \rangle_\lambda \langle B_1 \rangle_\lambda \langle A_2 \rangle_\lambda \langle B_2 \rangle_\lambda \\ &= \langle A_1 \rangle_\lambda \langle B_1 \rangle_\lambda (1 \pm \langle A_2 \rangle_\lambda \langle B_2 \rangle_\lambda) - \\ &\quad \langle A_1 \rangle_\lambda \langle B_2 \rangle_\lambda (1 \pm \langle A_2 \rangle_\lambda \langle B_1 \rangle_\lambda)\end{aligned}$$

Since $|\langle A_x \rangle_\lambda| \leq 1$ and $|\langle B_y \rangle_\lambda| \leq 1$, we have

$$|\langle A_1 B_1 \rangle - \langle A_1 B_2 \rangle| \leq \int_{\Lambda} d\lambda q(\lambda) (1 \pm \langle A_2 \rangle_\lambda \langle B_2 \rangle_\lambda) + \int_{\Lambda} d\lambda q(\lambda) (1 \pm \langle A_2 \rangle_\lambda \langle B_1 \rangle_\lambda)$$



CHSH inequality

1 Bell nonlocality

By using $\int_{\Lambda} d\lambda q(\lambda) = 1$, we have:

$$|\langle A_1B_1 \rangle - \langle A_1B_2 \rangle| \leq 2 \pm \left(\int_{\Lambda} d\lambda q(\lambda) \langle A_2 \rangle_{\lambda} \langle B_2 \rangle_{\lambda} + \int_{\Lambda} d\lambda q(\lambda) \langle A_2 \rangle_{\lambda} \langle B_1 \rangle_{\lambda} \right)$$

These integration must be positive, and we have:

$$|\langle A_1B_1 \rangle - \langle A_1B_2 \rangle| \leq 2 - (\langle A_2B_2 \rangle + \langle A_2B_1 \rangle)$$

Finally, we get the CHSH inequality:

$$|\langle A_1B_1 \rangle - \langle A_1B_2 \rangle + \langle A_2B_2 \rangle + \langle A_2B_1 \rangle| \leq 2$$

J. Clauser *et al.*, Phys.Rev.Lett. 23 (1969) 880-884



CHSH inequality

1 Bell nonlocality

In many literature, A_x and B_y are chosen as measurements of the spin of two qubits:

$$A_x = \vec{a}_x \cdot \vec{\sigma}, \quad B_y = \vec{b}_y \cdot \vec{\sigma},$$

where \vec{a}_x and \vec{b}_y are four unit vectors of the measurement axes. The CHSH inequality is rewritten to:

$$|\langle \vec{a}_1 \cdot \vec{\sigma} \otimes \vec{b}_1 \cdot \vec{\sigma} \rangle - \langle \vec{a}_1 \cdot \vec{\sigma} \otimes \vec{b}_2 \cdot \vec{\sigma} \rangle + \langle \vec{a}_2 \cdot \vec{\sigma} \otimes \vec{b}_2 \cdot \vec{\sigma} \rangle + \langle \vec{a}_2 \cdot \vec{\sigma} \otimes \vec{b}_1 \cdot \vec{\sigma} \rangle| \leq 2$$



Two-qubit system

1 Bell nonlocality

The fundamental quantity that describes the two-qubit system is the density matrix. It is parameterized in the global Hilbert space with 16 matrices $\{\mathbb{1}_2^A, \sigma_1^A, \sigma_2^A, \sigma_3^A\} \otimes \{\mathbb{1}_2^A, \sigma_1^A, \sigma_2^A, \sigma_3^A\}$:

$$\rho = \frac{1}{4} \left(\mathbb{1}_2 \otimes \mathbb{1}_2 + \sum_i B_i^+ \sigma_i \otimes \mathbb{1}_2 + \sum_j B_j^- \mathbb{1}_2 \otimes \sigma_j + \sum_{ij} C_{ij} \sigma_i \otimes \sigma_j \right),$$

where B_i^+ is the net polarization of the first qubit, while B_j^- is the net polarization of the second qubit. C_{ij} is the element of the spin correlation matrix.

U. Fano, Rev.Mod.Phys. 55 (1983) 855-874



Two-qubit system

1 Bell nonlocality

Implementing this density matrix to the calculation of expectations:

$$\langle A_x B_y \rangle = \text{Tr} [\rho (\vec{a}_x \cdot \vec{\sigma} \otimes \vec{b}_y \cdot \vec{\sigma})] = \sum_{ij} C_{ij} a_{x,i} b_{y,j}.$$

Now the CHSH inequality can be expressed as

$$|\vec{a}_1^T C (\vec{b}_1 - \vec{b}_2) + \vec{a}_2^T C (\vec{b}_1 - \vec{b}_2)| \leq 2.$$

The maximum of the left hand side is given by:

$$\max |\vec{a}_1^T C (\vec{b}_1 - \vec{b}_2) + \vec{a}_2^T C (\vec{b}_1 - \vec{b}_2)| = 2\sqrt{\lambda_1 + \lambda_2},$$

where λ_1 and λ_2 are the largest eigenvalues of $C^T C$.

R. Horodecki *et al.*, Phys.Lett.A 200 (1995) 5, 340-344



Two-qubit system

1 Bell nonlocality

In particular, we can choose

$$\vec{a}_1 = (0, 0, 1), \quad a_2 = (1, 0, 0), \\ \vec{b}_1 = (\pm \frac{1}{\sqrt{2}}, 0, \pm \frac{1}{\sqrt{2}}), \quad \vec{b}_2 = (\pm \frac{1}{\sqrt{2}}, 0, \mp \frac{1}{\sqrt{2}})$$

The CHSH inequality becomes:

$$\mathcal{B}_{\pm} = |C_{33} \pm C_{11}| < \sqrt{2}$$

\mathcal{B}_{\pm} is called Bell variable.

J.A. Aguilar-Saavedra *et al.*, arXiv:2205.00542



Two-qubit system

1 Bell nonlocality

The another important variable is called concurrence, which is given by

$$\mathcal{C}(\rho) = \max(0, \nu_1 - \nu_2 - \nu_3 - \nu_4),$$

where ν_i are the eigenvalues, with descendent order, of the operator

$$R = \sqrt{\sqrt{\rho}\tilde{\rho}\sqrt{\rho}} \quad \text{with} \quad \tilde{\rho} = (\sigma_y \otimes \sigma_y)\rho^*(\sigma_y \otimes \sigma_y).$$

Separable states have $\mathcal{C}(\rho) = 0$, while entangle states have $0 < \mathcal{C}(\rho) \leq 1$.

W. Wootters, arXiv:quant-ph/9709029



Table of Contents

2 Methodology

► Bell nonlocality

► Methodology

► Collider studies

► Summary



The Decay Approach

2 Methodology

When a particle decays, its daughter a has an associated spin analyzing power κ^a that quantifies the correlation between the daughter and the mother. θ_i^a represents the angle between the 3-momentum of daughter a and the axis i in the rest frame of the mother.

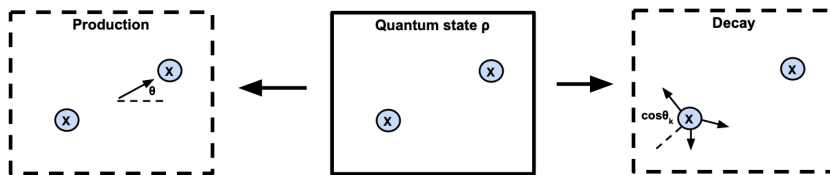


FIG. 1. Schematic illustration for a quantum state described by the density matrix ρ at the center, that may be probed by the production kinematics or by the angular variables of the decay products.



The Decay Approach

2 Methodology

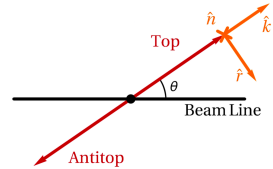
The distributions of θ_i^a can give:

$$B_i^+ = \frac{3}{\kappa^a} \langle \cos \theta_i^a \rangle, \quad B_j^+ = \frac{3}{\kappa^b} \langle \cos \theta_j^b \rangle$$
$$C_{ij} = -\frac{9}{\kappa_a \kappa_b} \langle \cos \theta_i^a \cos \theta_j^b \rangle$$

A convenient choice of axes is

$$\hat{k} = \text{top direction}, \quad \hat{r} = \frac{\hat{p} - \hat{k} \cos \theta}{\sin \theta}, \quad \hat{n} = \hat{k} \times \hat{r},$$

where \hat{p} is the beam axis. $i, j \in \{k, r, n\}$





The Kinematic Approach

2 Methodology

The density matrix can be parameterized by the scattering angle Θ between the incoming and outgoing particle and the speed β of the center-of-mass frame of the two-qubit system:

$$\rho = \rho(\Theta, \beta)$$

This is process-dependent. For the $q\bar{q} \rightarrow t\bar{t}$ process, the correlation matrix is

$$C_{ij} = \begin{pmatrix} \frac{2c_\Theta^2 + \beta^2 s_\Theta^2}{2 - \beta^2 s_\Theta^2} & 0 & -\frac{2c_\Theta s_\Theta \sqrt{1 - \beta^2}}{2 - \beta^2 s_\Theta^2} \\ 0 & \frac{-\beta^2 s_\Theta^2}{2 - \beta^2 s_\Theta^2} & 0 \\ -\frac{2c_\Theta s_\Theta \sqrt{1 - \beta^2}}{2 - \beta^2 s_\Theta^2} & 0 & \frac{(2 - \beta^2)s_\Theta^2}{2 - \beta^2 s_\Theta^2} \end{pmatrix}$$

, where $c_\Theta = \cos \Theta$ and $s_\Theta = \sin \Theta$.



Table of Contents

3 Collider studies

► Bell nonlocality

► Methodology

► Collider studies

► Summary



$e^+e^- \rightarrow q\bar{q}$ [K. Cheng and B. Yan, arXiv:2501.03321]
3 Collider studies

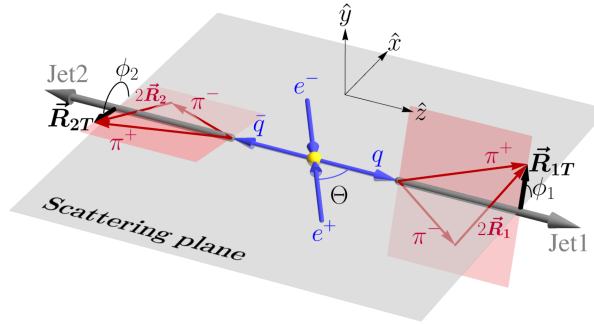


FIG. 1. Leading order kinematic configuration of $\pi^+\pi^-$ dihadron pair production at lepton colliders.



$$e^+ e^- \rightarrow q\bar{q} \text{ [K. Cheng and B. Yan, arXiv:2501.03321]}$$

3 Collider studies

With the axis they choose, the Bell variable is

$$\mathcal{B}_\pm = |C_{xx} \pm C_{yy}|.$$

The correlation matrix is

$$C_{ij} = \text{diag} \left(\frac{\sin^2 \Theta}{1 + \cos^2 \Theta}, \frac{\sin^2 \Theta}{1 + \cos^2 \Theta}, 1 \right),$$

where Θ is the scattering angle. The net polarization vectors of quarks are zero, which means $B_i^+ = B_j^- = 0$. Then the Bell variables are

$$\mathcal{B}_+ = 0, \quad \mathcal{B}_- = \frac{2 \sin^2 \Theta}{1 + \cos^2 \Theta}$$



$e^+e^- \rightarrow q\bar{q}$ [K. Cheng and B. Yan, arXiv:2501.03321]

3 Collider studies

$$\mathcal{B}_- = \frac{2\langle \cos(\phi_1 + \phi_2) \rangle}{\alpha_{M_1, M_2}^{z_1, z_2}} = \frac{A_{12}}{\alpha_{M_1, M_2}^{z_1, z_2}},$$

where $\alpha_{M_1, M_2}^{z_1, z_2}$ is the analyzing power. In this paper, the quark momenta are k_1, k_2 . The corresponding momenta of pion pair are P_1, P_2 . $P_i^\pm(k_i^\pm)$ represents their light-cone components. $z_1 = P_1^-/k_1^-$ and $z_2 = P_2^+/k_2^+$.

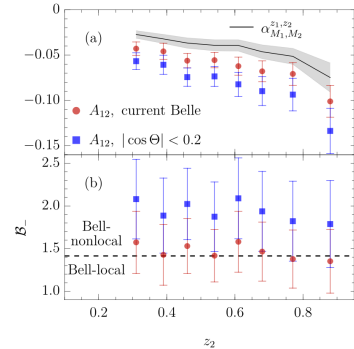


FIG. 2. (a) The current measurement of A_{12} (red points) and expected measurement of A_{12} with a selection cut of $|\cos \Theta| < 0.2$ (blue points), together with the spin analyzing power $\alpha_{M_1, M_2}^{z_1, z_2}$ (black line) calculated with JAMDiFF [42, 43]. (b) The Bell variable $\mathcal{B}_- = A_{12}/\alpha_{M_1, M_2}^{z_1, z_2}$, reconstructed from current data set (red) and expected data with a selection cut of $|\cos \Theta| < 0.2$ (blue).



$e^+e^- \rightarrow q\bar{q}$ [K. Cheng and B. Yan, arXiv:2501.03321]
3 Collider studies

- With 100% correlated systematic uncertainties, the significance is 2.5σ .
- With 0% correlated systematic uncertainties, the significance exceeds 5σ .

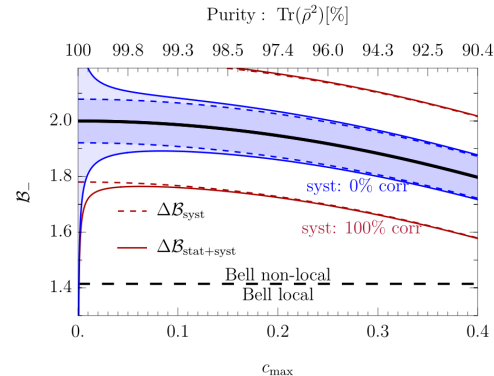


FIG. 3. Expected result of $\mathcal{B}_- \pm \Delta\mathcal{B}$ as a function of selection cut $|\cos\Theta| < c_{\max}$, assuming the systematical uncertainties in each bin are uncorrelated (blue) or 100% correlated (red).



$$e^+ e^- \rightarrow \tau^+ \tau^- \quad [\text{T. Han } et al., \text{ arXiv:2501.04801}]$$

3 Collider studies

This paper studies $e^+ e^- \rightarrow \tau^+ \tau^-$ at BEPC-II, where $\sqrt{s} \ll m_Z$. The spin correlation matrix is simplified to:

$$C_{ij} = \frac{1}{2 - \beta^2 \sin^2 \theta} \begin{pmatrix} (2 - \beta^2) \sin^2 \theta & 0 & \sqrt{1 - \beta^2} \sin 2\theta \\ 0 & -\beta^2 \sin^2 \theta & 0 \\ \sqrt{1 - \beta^2} \sin 2\theta & 0 & \beta^2 + (2 - \beta^2) \cos^2 \theta \end{pmatrix},$$

K. Ehatäh et al., arXiv:2311.17555

where β is the velocity in the center-of-mass frame of τ , and θ is the scattering angle. In this low energy, the concurrence has a simplified form:

$$\mathcal{C} = \frac{1}{2} (C_{11} + C_{33} - C_{22} - 1).$$



$e^+e^- \rightarrow \tau^+\tau^-$ [T. Han *et al.*, arXiv:2501.04801]
3 Collider studies

With the kinematic approach, the concurrence \mathcal{C} and the Bell variable \mathcal{B} are

$$\mathcal{C} = \frac{\beta^2 \sin^2 \theta}{2 - \beta^2 \sin^2 \theta}, \quad \mathcal{B} = 2 \sqrt{1 + \left(\frac{\beta^2 \sin^2 \theta}{2 - \beta^2 \sin^2 \theta} \right)^2}$$

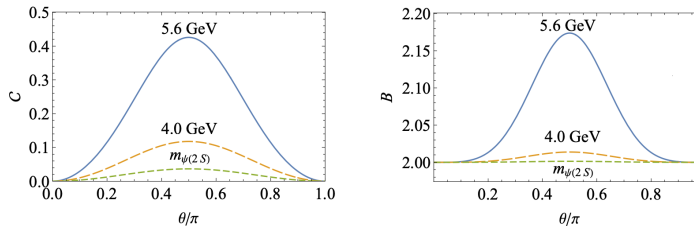


FIG. 3: The concurrence (left) and Bell variable (right) as a function of scattering angle θ at the center-of-mass energies of $\sqrt{s} = m_{\psi(2S)} = 3.7$ GeV, $\sqrt{s} = 4.0$ GeV, and $\sqrt{s} = 5.6$ GeV.



$e^+e^- \rightarrow \tau^+\tau^-$ [T. Han *et al.*, arXiv:2501.04801]
3 Collider studies

| Decay channel | | Branching fraction (%) | Spin analyzing power |
|------------------------------|----------|------------------------|----------------------|
| $\nu_\tau\pi^-$ | π^- | 10.8 | -1.00 |
| $\nu_\tau\rho^-$ | ρ^- | 25.2 | 0.45 |
| $\nu_\tau\pi^-\pi^+\pi^-$ | π^+ | 9.3 | 0.15 |
| $\nu_\tau\pi^-\pi^+\pi^-$ | π^- | 9.3 | 0.04 |
| $\nu_\tau\mu^-\bar{\nu}_\mu$ | μ^- | 17.4 | 0.34 |
| $\nu_\tau e^-\bar{\nu}_e$ | e^- | 17.8 | 0.34 |

TABLE I: The branching fractions and spin analyzing powers of the leading τ decay modes.

The spin analyzing power is given by the differential decay of τ in its rest frame:

$$\frac{1}{\Gamma} \frac{d\Gamma}{d \cos \theta_d} = \frac{1}{2} (1 + P \kappa \cos \theta_d),$$

where P is the polarization of τ , and θ_d is the angle between the decayed product and the polarization axis of τ in the rest frame of τ .



$e^+e^- \rightarrow \tau^+\tau^-$ [T. Han *et al.*, arXiv:2501.04801]
3 Collider studies

Only the $\nu_\tau\pi$ channel is considered in this paper.

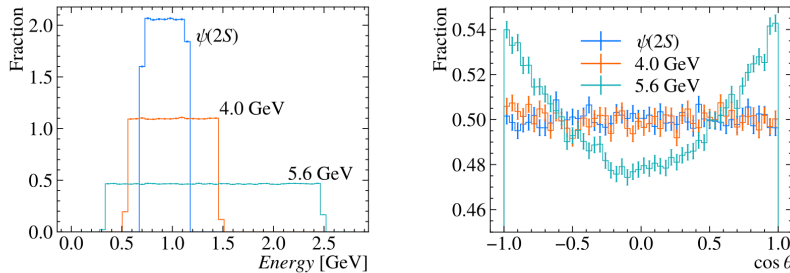


FIG. 2: The energy spectrum (left) and angular distribution (right) of π^\pm from the decays
 $\tau^- \rightarrow \nu_\tau\pi^-$ and $\tau^+ \rightarrow \bar{\nu}_\tau\pi^+$.



$$e^+ e^- \rightarrow \tau^+ \tau^- \quad [\text{T. Han et al., arXiv:2501.04801}]$$

3 Collider studies

The significances of \mathcal{C} and \mathcal{B} are defined as

$$\mathcal{S}(\mathcal{C}) = \frac{\mathcal{C}}{\sqrt{(\Delta\mathcal{C}_{\text{stat}})^2 + (\Delta\mathcal{C}_{\text{sys}})^2}}, \quad \mathcal{S}(\mathcal{B}) = \frac{\mathcal{B} - 2}{\sqrt{(\Delta\mathcal{B}_{\text{stat}})^2 + (\Delta\mathcal{B}_{\text{sys}})^2}},$$

where the systematic uncertainty is

$$\Delta_{\text{sys}} = \{0.5\%, 1\%, 2\%, 5\%\}$$

The statistical uncertainty $\Delta_{\text{stat}} = k/\sqrt{N}$, where N is the number of reconstructed events. Two approaches have different prefactor k , which are calculated in [K. Cheng et al., arXiv:2410.08303]. The authors claim that the statistical uncertainty of kinematic approach is much smaller than the decay approach.



$e^+e^- \rightarrow \tau^+\tau^-$ [T. Han *et al.*, arXiv:2501.04801]
3 Collider studies

| Method | Δ_{sys} | \mathcal{C} | $\Delta\mathcal{C}_{\text{tot}}$ | $\mathcal{S}(\mathcal{C})$ | $\Delta\theta$ | $\mathcal{B}-2$ | $\Delta\mathcal{B}_{\text{tot}}$ | $\mathcal{S}(\mathcal{B})$ | $\Delta\theta$ |
|--------|-----------------------|---------------|----------------------------------|----------------------------|----------------|-----------------|----------------------------------|----------------------------|----------------|
| Decay | 0 | 0.029 | 0.020 | 1.42 | 100° | 0.0011 | 0.41 | 0.0026 | 2.3° |
| | 0.5% | 0.029 | 0.021 | 1.42 | 100° | 0.0011 | 0.41 | 0.0026 | 2.3° |
| | 1% | 0.029 | 0.021 | 1.40 | 100° | 0.0011 | 0.41 | 0.0026 | 2.3° |
| | 2% | 0.029 | 0.022 | 1.33 | 100° | 0.0011 | 0.42 | 0.0026 | 2.3° |
| | 5% | 0.029 | 0.029 | 1.02 | 100° | 0.0011 | 0.42 | 0.0025 | 2.2° |
| Kinem. | 0.5% | 0.037 | 0.0025 | > 5 σ , 7% | 0 | 0.0013 | 0.010 | 0.13 | 0 |
| | 1% | 0.037 | 0.0050 | > 5 σ , 14% | 0 | 0.0013 | 0.020 | 0.067 | 0 |
| | 2% | 0.037 | 0.010 | 3.70 | 0 | 0.0013 | 0.040 | 0.033 | 0 |
| | 5% | 0.037 | 0.025 | 1.46 | 0 | 0.0013 | 0.10 | 0.013 | 0 |

TABLE II: The significance of observing entanglement and Bell nonlocality in the current $\psi(2S)$ dataset for the benchmark values of the systematic uncertainties Δ_{sys} , with the efficiency and cuts specified in Sec. III B. When the optimal angular window is smaller than 5°, we use the non-optimal value of 5°. When the significance is greater than 5 σ we show the expected precision of the measurement \mathcal{S}^{-1} .

$\Delta\theta$ is a cut for scattering angle $|\theta - \pi/2| < \Delta\theta/2$.



$e^+e^- \rightarrow \tau^+\tau^-$ [T. Han *et al.*, arXiv:2501.04801]
3 Collider studies

| Method | Δ_{sys} | \mathcal{C} | $\Delta\mathcal{C}$ | $\mathcal{S}(\mathcal{C})$ | $\Delta\theta$ | $\mathcal{B}-2$ | $\Delta\mathcal{B}$ | $\mathcal{S}(\mathcal{B})$ | $\Delta\theta$ |
|--------|-----------------------|---------------|---------------------|----------------------------|----------------|-----------------|---------------------|----------------------------|----------------|
| Decay | 0 | 0.21 | 0.034 | $> 5\sigma$, 16% | 96° | 0.058 | 0.026 | 2.3 | 17° |
| | 0.5% | 0.21 | 0.035 | $> 5\sigma$, 16% | 95° | 0.060 | 0.028 | 2.1 | 16° |
| | 1% | 0.21 | 0.035 | $> 5\sigma$, 16% | 95° | 0.062 | 0.034 | 1.9 | 15° |
| | 2% | 0.21 | 0.036 | $> 5\sigma$, 17% | 94° | 0.066 | 0.050 | 1.3 | 12° |
| | 5% | 0.22 | 0.043 | $> 5\sigma$, 20% | 86° | 0.070 | 0.10 | 0.67 | 7° |
| Kinem. | 0 | 0.26 | 0.0010 | $> 5\sigma$, 0.39% | 45° | 0.062 | 0.00018 | $> 5\sigma$, 0.29% | 15° |
| | 0.5% | 0.26 | 0.0029 | $> 5\sigma$, 1.1% | 39° | 0.073 | 0.0097 | $> 5\sigma$, 13% | 1.2° |
| | 1% | 0.26 | 0.0054 | $> 5\sigma$, 2.0% | 31° | 0.073 | 0.019 | 3.8 | 0.77° |
| | 2% | 0.27 | 0.011 | $> 5\sigma$, 4.0% | 21° | 0.073 | 0.039 | 1.9 | 0.49° |
| | 5% | 0.27 | 0.027 | $> 5\sigma$, 9.9% | 12° | 0.073 | 0.097 | 0.75 | 0.26° |

TABLE IV: The significance of observing entanglement and Bell nonlocality in the future 4.0 – 5.6 GeV dataset for the benchmark values of the systematic uncertainties Δ_{sys} , with the efficiency and cuts specified in Sec. III B. When the optimal angular window is smaller than 10°, we use the non-optimal value of 10°. When the significance is greater than 5σ we show the expected precision of the measurement \mathcal{S}^{-1} .



$e^+e^- \rightarrow \tau^+\tau^-$ [T. Han *et al.*, arXiv:2501.04801]
3 Collider studies

| Method | Δ_{sys} | \mathcal{C} | $\Delta\mathcal{C}$ | $\mathcal{S}(\mathcal{C})$ | $\Delta\theta$ | $\mathcal{B}-2$ | $\Delta\mathcal{B}$ | $\mathcal{S}(\mathcal{B})$ | $\Delta\theta$ |
|--------|-----------------------|---------------|---------------------|----------------------------|----------------|-----------------|---------------------|----------------------------|----------------|
| Decay | 0 | 0.21 | 0.034 | $> 5\sigma$, 16% | 96° | 0.058 | 0.026 | 2.3 | 17° |
| | 0.5% | 0.21 | 0.035 | $> 5\sigma$, 16% | 95° | 0.060 | 0.028 | 2.1 | 16° |
| | 1% | 0.21 | 0.035 | $> 5\sigma$, 16% | 95° | 0.062 | 0.034 | 1.9 | 15° |
| | 2% | 0.21 | 0.036 | $> 5\sigma$, 17% | 94° | 0.066 | 0.050 | 1.3 | 12° |
| | 5% | 0.22 | 0.043 | $> 5\sigma$, 20% | 86° | 0.070 | 0.10 | 0.67 | 7° |
| Kinem. | 0 | 0.26 | 0.0010 | $> 5\sigma$, 0.39% | 45° | 0.062 | 0.00018 | $> 5\sigma$, 0.29% | 15° |
| | 0.5% | 0.26 | 0.0029 | $> 5\sigma$, 1.1% | 39° | 0.073 | 0.0097 | $> 5\sigma$, 13% | 1.2° |
| | 1% | 0.26 | 0.0054 | $> 5\sigma$, 2.0% | 31° | 0.073 | 0.019 | 3.8 | 0.77° |
| | 2% | 0.27 | 0.011 | $> 5\sigma$, 4.0% | 21° | 0.073 | 0.039 | 1.9 | 0.49° |
| | 5% | 0.27 | 0.027 | $> 5\sigma$, 9.9% | 12° | 0.073 | 0.097 | 0.75 | 0.26° |

TABLE IV: The significance of observing entanglement and Bell nonlocality in the future 4.0 – 5.6 GeV dataset for the benchmark values of the systematic uncertainties Δ_{sys} , with the efficiency and cuts specified in Sec. III B. When the optimal angular window is smaller than 10° , we use the non-optimal value of 10° . When the significance is greater than 5σ we show the expected precision of the measurement \mathcal{S}^{-1} .



$e^+e^- \rightarrow \tau^+\tau^-$ [T. Han *et al.*, arXiv:2501.04801]
3 Collider studies

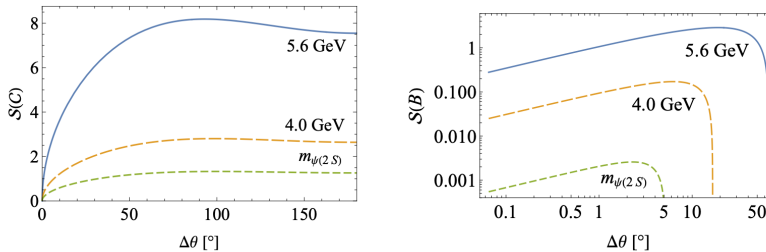


FIG. 4: The significance of the concurrence (left) and Bell variable (right) with the decay method as a function of the size of the angular window $\Delta\theta$ at the center-of-mass energies of $\sqrt{s} = m_{\psi(2S)} = 3.7$ GeV, $\sqrt{s} = 4.0$ GeV, and $\sqrt{s} = 5.6$ GeV using the decay method with the $\nu\pi$ decay channel and the integrated luminosity $L = 20 \text{ fb}^{-1}$ for $\sqrt{s} = 4.0$ GeV and $\sqrt{s} = 5.6$ GeV and $N_{\psi(2S) \rightarrow \tau^+\tau^-} = 3.5 \times 10^6$ for $\sqrt{s} = m_{\psi(2S)}$. The systematic uncertainty Δ_{sys} is not included.



$e^+e^- \rightarrow \tau^+\tau^-$ [T. Han *et al.*, arXiv:2501.04801]
3 Collider studies

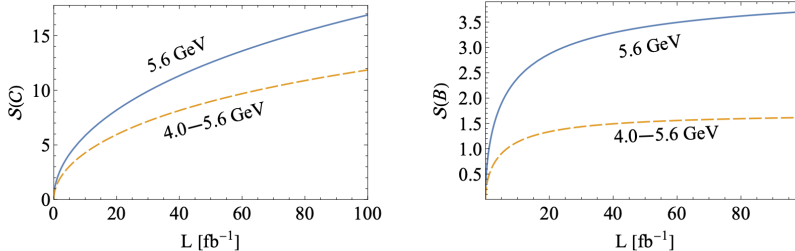


FIG. 5: The optimal significance of observing entanglement (left) and Bell inequality violation (right) as a function of integrated luminosity at 5.6 GeV and 4.0 – 5.6 GeV using the decay method in the $\nu\pi$ channel and $\Delta_{\text{sys}} = 2\%$. The angular window cut is optimized at $L = 20 \text{ fb}^{-1}$ and used for all luminosity values.



Table of Contents

4 Summary

► Bell nonlocality

► Methodology

► Collider studies

► Summary



Summary

4 Summary

- The basic knowledge of Bell nonlocality is reviewed
- Two approaches can be applied to study the Bell nonlocality: decay approach and kinematic approach.
- Two collider studies are reviewed: $e^+e^- \rightarrow q\bar{q}$ and $e^+e^- \rightarrow \tau^+\tau^-$.



Q&A

*Thank you for listening!
Your feedback will be highly appreciated!*